OPTIMIZING THE UNIT STRUCTURE OF THE DRAINAGE-TYPE CYCLONE SEPARATOR FOR SAND SAMPLE COLLECTION
/
优化排水型旋风分离砂样采集器的单元结构

Caoqi ZHANG [1)], Muhammad Ariff Bin BAHARUDIN[1*)], Taiming GUO [2)], Jining ZHANG [3)], Shiping WU [4)]
[1)] Faculty of Electrical Engineering, Universiti Teknologi Malaysia, Johor Skudai/Malaysia
[2)] Faculty of Computer Engineering, Universiti Teknologi Malaysia, Johor Skuda/Malaysia
[3)] State Nuclear Electric Power Planning Design & Research Institute, Beijing/China
[4)] Faculty of Humanities and Social Sciences, Datong No.12 Middle School Shanxi, 034400, P.R. China
Tel: +60172178749; E-mail: mariff@utm.my
Corresponding author: Muhammad Ariff Bin Banharudin
DOI: https://doi.org/10.35633/inmateh-74-55

Keywords: *Sand sampler, sampling efficiency, orthogonal experiment, regression model, wind erosion*

ABSTRACT
This paper introduces a cyclone separation sand sampler with diversion flow to enhance soil wind erosion monitoring accuracy. Using CFD simulations and orthogonal testing, the optimal structural parameters for improved sampling efficiency were determined. A response model showed strong predictive capability with a P-value less than 0.0001 and R^2 of 0.9482. Wind tunnel tests demonstrated that the new sampler achieved a 91.44% efficiency, surpassing the 90.81% of the traditional design. The research provides valuable data for more accurate wind-sand flow monitoring, aiding in desertification prevention and improving wind erosion assessments in grasslands.

摘要
本文介绍了一种带有导流装置的旋风分离式沙尘采样器，以提高土壤风蚀监测的精度。通过 CFD 仿真和正交试验，确定了优化后的结构参数以提高采样效率。响应模型显示其预测能力较强，P 值小于 0.0001，R^2为 0.9482。风洞试验结果表明，新型采样器的采样效率达到91.44%，高于传统设计的90.81%。该研究为更准确的风沙流监测提供了有价值的数据参考，有助于防治荒漠化并改善草原风蚀评估。

INTRODUCTION
In recent years, nearly 180 million hectares of grasslands have undergone severe degradation. The degradation phenomenon has led to a continuous decline in grassland quality *(Song, 2016)*. Soil wind erosion is the main factor causing grassland degradation, which is jointly restricted by climate, soil, vegetation, and human factors *(Jhang et al., 2019)*. The sand sampler is a type of wind erosion testing device, which is employed to measure the quantity of sand transported in the wind-sand flow and the wind-sand flow and the structure of the wind-sand flow *(Liu et al., 2019; Li et al., 2022)*. It is an indispensable instrument for studying soil wind erosion and grassland degradation and observing the structural characteristics of wind sand flow in indoor and outdoor wind tunnels *(Khan et al. et al., 2021)*.

Recently, domestic scholars have conducted extensive research on the sampling efficiency of the internal flow field of sand sampler units using aerodynamic (CFD) principles for different sand sampler devices *(Petrichenko, 2020*). The CFD method was used to study the internal velocity flow field and the principle of velocity reduction of the diversion counter flow sand sampler *(Song et al., 2018)*. The coupling method of CFD and the discrete element method were used to study and analyze the motion of gas-solid two-phase flow in a sand sampler *(Yang, 2021).* The CFD method was used to study the relationship between the internal velocity flow field and size parameters of a cyclone separation sand sampler unit *(Huang et al., 2015)*. In the case of the existing cyclone separation sand sampler, the sampler method of particles has not been researched. The use of sandbags and sandboxes to collect particles has also resulted in a significant reduction in the velocity of airflow backflow inside the sampler box, becoming the main reason for affecting the sampling efficiency. Based on this, a drainage method has been proposed in this article to make particles in the drainage tube only affected by gravity, reducing the reflux speed of the airflow, and thereby, the sampling efficiency of the sand sampler will be improved *(Chen et al., 2018)*.

A cyclone separation sand sampler of drainage type was designed, and the mathematical model between the sampling efficiency, structural parameters, and airflow velocity of its sand sampler unit was studied in this paper *(Yan et al., 2024)*. Firstly, the velocity and flow field of the sand sampler unit was simulated, and Design Expert software was used to design the sampling efficiency experiment *(Xu et al., 2023; Dumitru et al., 2024)*. Secondly, the experimental data was classified and statistically analyzed, and a sampling efficiency response model using orthogonal experimental methods was established. Finally, the effects of the structural parameters of the sand sampler unit, airflow velocity, and their interaction on sampling efficiency were studied, providing corresponding theoretical references for the design and structural optimization of the drainage-type cyclone separation sand sampler *(Zhang et al., 2023; He et al., 2024*).

To summarize, in recent years, approximately 180 million hectares of grasslands have suffered severe degradation, primarily caused by soil wind erosion, which is influenced by climate, soil, vegetation, and human factors. The sand sampler, as a key device for measuring sand transport volume and wind-sand flow structure, is widely used in the study of soil wind erosion and grassland degradation. Existing research mainly focuses on improving the sampling efficiency of the internal flow field of sand samplers using CFD methods. This paper proposes a drainage-based cyclone separation sand sampler to reduce airflow reflux speed and improve sampling efficiency, providing theoretical references for the design and structural optimization of drainage-type sand samplers.

MATERIALS AND METHODS

Drainage type sand sampler unit

The system is divided into two plate assemblies, a field terminal, and a remote client. The system's overall framework is shown in Fig. 1, and its appearance is shown in Fig. 2.

At present, drainage and sampler treatment on the particles after gas-solid sampling has not been conducted in the cyclone separation type sand sampler research. In order to improve the sampling efficiency, this study focuses on optimizing the drainage tube, which is connected to the sand sampler unit using PVC rigid pipes, as shown in Figure 1. The left side of the sand flow enters from the air inlet. In the sand sampler unit, the purified gas is discharged from the upper exhaust funnel, and particles are collected from the lower sand discharge port. The direction of movement of the airflow and particles is the same. Through drainage, the reflux speed of the airflow is reduced, thereby improving the sampling efficiency of the sand sampler unit.

The research process was conducted through CFD simulation to analyze the velocity flow field of the drainage and traditional sand sampler units, as shown in Figure 2. The flow velocity field reflects the changes in particle motion velocity within the sand sampler unit. The smaller the velocity near the exhaust pipe, the fewer particles escaped, thus verifying the higher sampling efficiency *(Patil et al., 2022; Li, 2022)*.

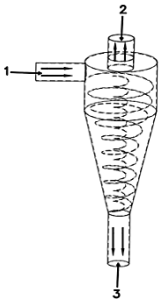

1. Air inlet 2. Exhaust outlet 3. Sand discharge outlet

Fig. 1 - Particle motion trajectory diagram

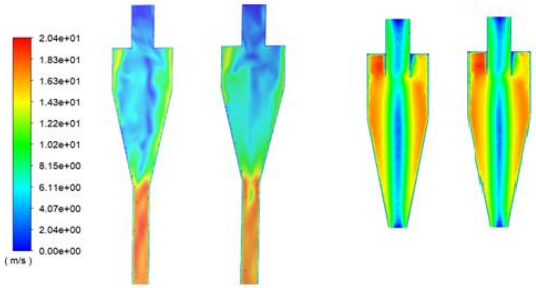

(a) Drainage type (b) Traditional type

Fig. 2 - Numerical simulation distribution diagram of velocity flow field

In the simulation experiment, the variable factor is wind speed, and the amount of particle injection at the inlet is set. When the residual calculation is completed, the corresponding velocity flow field and the capture and escape amount of particles are obtained. The sampling efficiency of the capture amount of particles, the injection amount, and the final particle capture amount are the standards for measuring the sampling efficiency. Simulation experiments have found that particles are significantly affected by gravitational acceleration in the drainage tube, reducing the impact of reflux on particles. The sampling efficiency of the drainage and traditional sand sampler units increases with the increase in wind speed, and the sampling efficiency of both types of sand sampler units shows an upward trend within 10-13 m/s. In an ideal state, the sampling efficiency of the drainage sand sampler unit can reach 100% at a wind speed of 13 m/s.

The sampling efficiency of traditional sand sampler units is 99.7%. As a result, the sampling efficiency of the cyclone separation sand sampler unit with an increased drainage tube is significantly higher than that of the cyclone sampling sand sampler unit without a drainage tube. The line chart in Figure 3 intuitively shows that the sampling efficiency of the drainage-type sand sampler unit is better than that of the traditional-type sand sampler unit. The calculation formula for sampling efficiency:

$$X = S_1 / S_2 \quad (1)$$

Formula (1) where S_1 is the sand sampler capacity, S_2 represents the sand transport capacity, X is the dispersion efficiency.

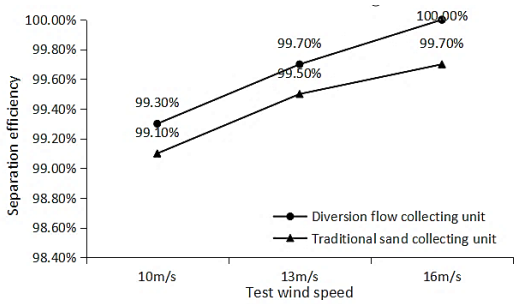

Fig. 3 - Comparison diagram of flow diversion and conventional sampling efficiency

Design optimization and result analysis of 2 drainage sand sampler units Overall Plan Design

Through simulation, adding a drainage tube to the sand sampler unit can improve the sand sampler rate of the cyclone separation sand sampler instrument. Regarding the factors that may affect the sampling efficiency of the sand sampler unit, the CFD simulation method was used to calculate the flow field of the drainage cyclone separation sand sampler unit. The effects of inlet wind speed (A), outlet diameter (B), exhaust pipe diameter (C), exhaust pipe insertion depth (D), cylinder section height (E), and cone section height (F) on the sampling efficiency of the sand sampler unit were studied. The interaction between different influencing factors was analyzed through orthogonal experiments.

A response model was established using the six-factor, three-level Box-Behnken response surface analysis method. The natural wind speed of sand lifting under natural conditions was 13.8 m/s, and the inlet wind speed in the orthogonal experiment, with values of 10 m/s, 13 m/s, and 16 m/s, was used as the reference wind speed for simulation. The level of experimental factors is shown in Table 1.

Table 1

Test factors and level of sampling efficiency

Test factors	Factor code	Factor level code		
		-1	0	1
Air inlet wind speed / (m/s)	A	10	13	16
Sand outlet diameter / mm	B	10	12.5	15
Exhaust funnel diameter / mm	C	20	25	30
Insertion depth of exhaust funnel / mm	D	0	10	20
Height of cylinder section / mm	E	40	50	60
Cone segment height / mm	F	80	90	100

Establishment and Regression Analysis

Design Expert software was used to establish a regression model for the influencing factors. Regression model variance analysis, R2 comprehensive analysis, and response surface analysis of the interaction between the influencing factors were conducted. The best parameter combination was obtained through the fitting degree of the model.

Multiple models were applied to model simulation data, and the model analysis results are shown in Table 2. The lower the P-value in the table (rejecting the original assumed value), the higher the fitting degree of the model. The F-value is a test of the fit of the regression equation, and the larger the value, the higher the fit of the model; R2 represents the fit test of the model on the data, and the closer its value is to 1, the higher the fit of the model. According to the data comparison and analysis results of multiple model variances in Table 2, the P values of the linear model, 2FI model, quadratic equation model, and cubic equation model are all less than 0.05, indicating that the model fitting is relatively significant. The f-values indicate that the fitting degree of the linear and quadratic models is better than that of the 2FI and cubic models.

The comprehensive analysis of R2 fitted by the four models in Table 3 shows that the R2 value of the quadratic equation model is 0.9980, the R2 value of the cubic equation model is 0.9482, both greater than 0.9, the R2 value of the linear model is 0.6428, and the R2 value of the 2FI model is 0.8004, both less than 0.9, indicating that the quadratic equation model and the cubic equation model have a high correlation with the test, and the model is more accurate. Based on the analysis results in Tables 2 and 3, a quadratic equation model was selected for the sampling efficiency response model.

Table 2

Analysis of variance of multiple regression models for sampling efficiency

Model type	Sum of squares	Free degree	Mean square value	F-value	P-value
Average value	48.82	1	48.82		
Linear	0.020	6	3.381E-003	19.69	< 0.0001
2FI	0.0241	15	1.607E-004	0.91	<0.0001
Quadratic equation	0.04192	6	6.986E-004	12.36	< 0.0001
Cubic equation	0.01411	18	7.842E-005	10.91	0.0009
residual	0.00575	8	7.187E-006		

Table 3

Square analysis of regression model R of sampling efficiency

Model type	Standard deviation	R2	R2 predicted value	Sum of squares of predicted residuals
Linear	0.013	0.7153	0.6428	0.010
2FI	0.013	0.8004	0.5477	0.013
Quadratic equation	7.517E-003	0.9980	0.7293	0.076
Cubic equation	2.681E-003	0.9482	0.4809	0.015

Table 4 shows the confidence analysis of the quadratic equation model and the influencing factors in the model. The estimated parameters of the factors in the table are the average values of the upper and lower values of the 95% confidence interval of the parameters, where VIF is the variable expansion factor, and the value between 0 and 10 is reasonable data for testing multicollinearity. Estimating the absolute value of parameters can infer the magnitude of the impact of each influencing factor on the response value. The results are: E>C>A>D>B>F (primary term), CD>DF>BC>AE>CE>AC>EF>AF>BD>BE>BF>CF>AB>AD>DE (interaction term of different factors), D2>E2>F2>B2>C2>A2 (secondary term), and the positive and negative values of the estimated parameters of each influencing factor can also indicate the direction of the response value, AC, AD, AE, AF, BD, BE, DE, DF, EF, A2, B2, C2, D2 E2 and F2 are adverse effects. In contrast, the other terms are positive effects. The positive effect is that the sampling efficiency increases with the increase of the independent variable, while the adverse effect is the opposite.

Table 4

Estimation of parameters of regression model of sampling efficiency

Factors	Estimating parameters	Free degree	Standard deviation	95% confidence interval		VIF
				Lower value	Upper value	
Domain	0.97	1	0.03069	0.97	0.98	
A	0.02667	1	0.01534	-0.00487	0.05821	1.00
B	0.02208	1	0.01534	-0.00945	0.05362	1.00
C	0.07042	1	0.01534	0.03888	0.010	1.00
D	0.026	1	0.01534	0.023	0.029	1.00
E	0.09292	1	0.01534	0.06138	0.012	1.00
F	0.01958	1	0.01534	-0.01196	0.05112	1.00
AB	0.01875	1	0.02658	-0.03588	0.07338	1.00
AC	-0.0475	1	0.02658	-0.010	0.07126	1.00
AD	-0.015	1	0.01879	-0.05363	0.02.363	1.00
AE	-0.0625	1	0.02658	-0.06088	0.04.838	1.00
AF	-0.04	1	0.02658	-0.0963	0.01463	1.00
BC	0.06625	1	0.02658	0.01162	0.012	1.00
BD	-0.00375	1	0.02658	-0.05838	0.05088	1.00

Factors	Estimating parameters	Free degree	Standard deviation	95% confidence interval		VIF
				Lower value	Upper value	
BE	-0.03125	1	0.01879	-0.06988	0.00738	1.00
BF	0.02875	1	0.02658	-0.02588	0.08338	1.00
CD	0.011	1	0.02658	0.05287	0.016	1.00
CE	0.05625	1	0.02658	0.00162	0.011	1.00
CF	0.02625	1	0.01879	-0.01238	0.06488	1.00
DE	-0.01375	1	0.02658	-0.06838	0.04088	1.00
DF	-0.0075	1	0.02658	-0.06213	0.04713	1.00
EF	-0.04375	1	0.02658	-0.09838	0.01088	1.00
A2	-0.03028	1	0.02344	-0.07845	0.01790	1.30
B2	-0.05819	1	0.02344	-0.011	-0.01002	1.30
C2	-0.04486	1	0.02344	-0.09304	0.00332	1.30
D2	-0.015	1	0.02344	-0.019	-0.09710	1.30
E2	-0.013	1	0.02344	-0.018	-0.08252	1.30
F2	-0.06736	1	0.02344	-0.012	-0.01919	1.30

RESULTS

Model validation

Before selecting the response model, each model's p-value and F-value R2 values were compared, and the quadratic equation model was validated through the residual standard probability plot of the model. As shown in Figure 4, the distribution of points on the residual average probability graph is approximately a straight line, with minor errors, indicating that the model is relatively reliable.

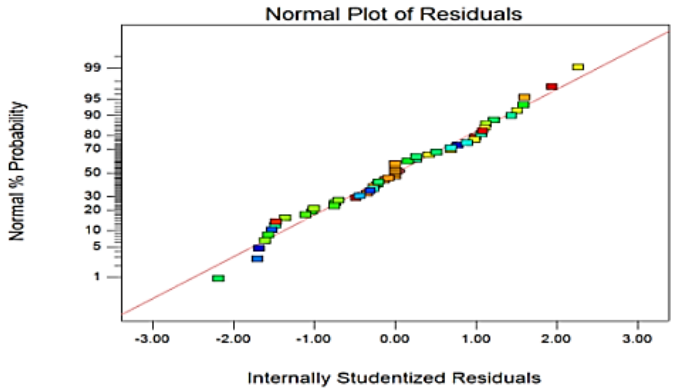

Fig. 4 - The student residual positive probability diagram of the sampling efficiency model

Analysis of Factors Influencing sampling Efficiency

The sand sampler's sampling efficiency is an important parameter for measuring the equipment's accuracy. A three-dimensional surface graph analyzed the interaction of six influencing factors on efficiency.

Figure 5 (a) shows the response surface of the interaction between the diameter of the sand outlet (B) and the inlet wind speed (A). When the diameter of the sand outlet is constant, the sampling efficiency increases with the increase of the inlet wind speed, with the maximum values being 0.72 and 0.962, respectively. The minimum wind speed for sand lifting is 13.8 m/s. When the diameter of the sand outlet increases from 10 mm to 12.5 mm, there is an insignificant upward trend in sampling efficiency. When the diameter of the sand outlet increases from 12.5 mm to 15 mm, there is an insignificant downward trend in sampling efficiency, and both have a small impact on sampling efficiency.

Figure 5 (b) shows the response surface of the interaction between the diameter of the exhaust funnel (C) and the inlet wind speed (A). When the diameter of the exhaust pipe is fixed, the sampling efficiency shows a significant increase and then a slow decrease with the increase in wind speed, with a maximum value of 0.97 and a minimum value of 0.955. When the inlet wind speed is constant, the sampling efficiency shows an insignificant trend of increasing and then decreasing with the increase of the exhaust pipe diameter, indicating that the exhaust pipe diameter has a particular impact on the sampling efficiency.

Figure 5 (c) shows the response surface of the interaction between the interpolation depth (D) of the exhaust funnel and the inlet wind speed (A). When the interpolation depth of the exhaust funnel is constant, the sampling efficiency shows a trend of slowly increasing and then slowly decreasing with the increase of the inlet wind speed, but its effect is insignificant. The highest sampling efficiency is 0.98, and the lowest is 0.976. When the inlet wind speed is constant, improving the sampling efficiency is achieved by changing the interpolation depth of the exhaust funnel. The sampling efficiency significantly increases when the interpolation depth of the exhaust funnel is between 0 mm and 15 mm but does not significantly decrease when the interpolation depth of the exhaust funnel is between 15 mm and 20 mm.

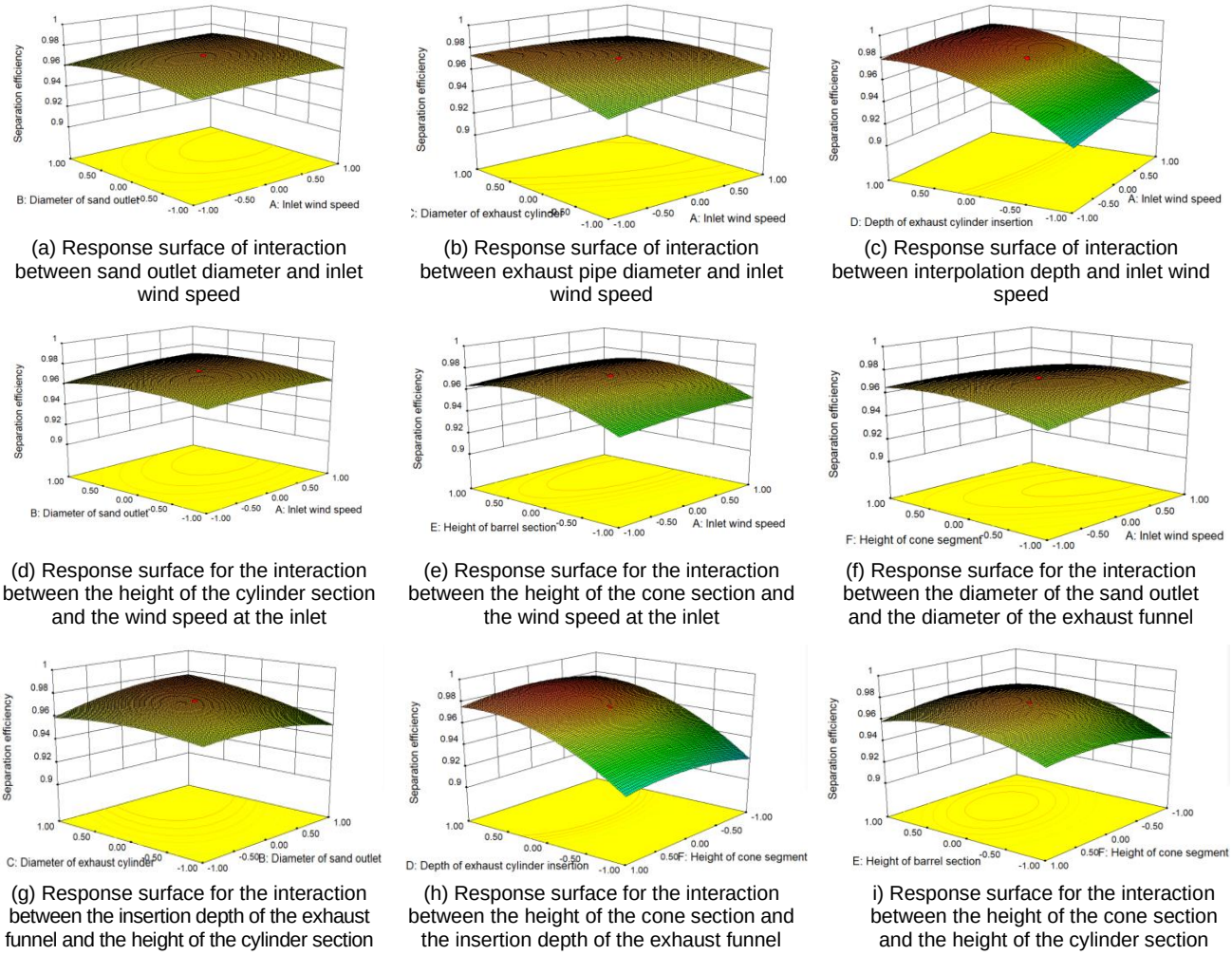

(a) Response surface of interaction between sand outlet diameter and inlet wind speed

(b) Response surface of interaction between exhaust pipe diameter and inlet wind speed

(c) Response surface of interaction between interpolation depth and inlet wind speed

(d) Response surface for the interaction between the height of the cylinder section and the wind speed at the inlet

(e) Response surface for the interaction between the height of the cone section and the wind speed at the inlet

(f) Response surface for the interaction between the diameter of the sand outlet and the diameter of the exhaust funnel

(g) Response surface for the interaction between the insertion depth of the exhaust funnel and the height of the cylinder section

(h) Response surface for the interaction between the height of the cone section and the insertion depth of the exhaust funnel

i) Response surface for the interaction between the height of the cone section and the height of the cylinder section

Fig. 5 - Response surface of second order interaction

Figure 5 (d) shows the response surface of the interaction between the height of the cylinder section (E) and the inlet wind speed (A). When the air inlet wind speed is constant, with the increase of the height of the cylinder section, the sampling efficiency shows a clear upward trend, while the downward trend is not apparent. The sampling efficiency reaches 0.974 when the cylinder section parameters reach 55 mm, and the sampling rate reaches 0.96 when the cylinder section parameters reach 60 mm. When the height of the cylinder section is constant, the increase in sampling efficiency is relatively small with the increase in wind speed, indicating that the influence of wind speed on sampling efficiency is significant.

Figure 5 (e) shows the response surface of the interaction between the height of the cone section (F) and the inlet wind speed (A). When the inlet wind speed is constant, the sampling efficiency slowly increases and then decreases with the increase of the height of the cone section. The height of the cone segment shows a significant upward trend within the range of 80 mm to 90 mm. When the inlet wind speed is constant, the sampling efficiency reaches its maximum value. When the height of the cone segment is 90 mm, the sampling efficiency can reach 0.965. The decrease in sampling efficiency is not significant within the range of 90 mm to 100 mm in the height of the cone section. When the height of the cone section is 100 mm, the sampling efficiency can reach 0.961. When the height of the cone section is constant, the sampling efficiency shows a trend of increasing and then decreasing with the increase of the inlet wind speed.

Figure 5 (f) shows the interaction response surface between the diameter of the sand outlet (B) and the diameter of the exhaust funnel (C). The diameter of the exhaust funnel and the diameter of the sand outlet have a significant impact on the sampling efficiency. When the diameter of the sand outlet is constant, the sampling efficiency increases with the increase of the diameter of the exhaust pipe. When the diameter of the exhaust pipe is large, the sampling efficiency increases with the increase of the diameter of the sand outlet. When the diameter of the exhaust pipe is small, the sampling efficiency shows a trend of increasing and then decreasing with the increase in the diameter of the sand outlet. When the diameter of the exhaust funnel is 30 mm, and the diameter of the sand outlet is 10 mm, the sampling efficiency is 0.96. When the diameter of the sand outlet is 15 mm, the sampling efficiency can reach 0.978.

Figure 5 (g) shows the response surface of the interaction between the insertion depth (D) of the exhaust funnel and the height of the cylinder section (E). When the height of the cylinder section is constant, the sampling efficiency shows an upward trend as the insertion depth of the exhaust funnel increases. When the insertion depth of the exhaust funnel is 0 mm and 20 mm, the sampling efficiency is 0.925 and 0.978, respectively. When the insertion depth of the exhaust funnel is constant, the sampling efficiency shows a trend of rapidly increasing and then slowly decreasing as the height of the cylinder section increases.

Figure 5 (h) shows the response surface of the interaction between the height of the cone section (F) and the insertion depth of the exhaust funnel (D). When the insertion depth of the exhaust pipe is constant, the efficiency shows an upward trend with the increase in the height of the cone section. When the insertion depth of the exhaust funnel is 0 mm and 20 mm, the efficiency can reach 0.923 to 0.978. As the height of the cone section increases, the sampling efficiency shows a slow increase and then a slow decrease trend. As mentioned above, the insertion depth of the exhaust funnel is constant, and the sampling efficiency can reach 0.975 and 0.982 with heights of 80 mm and 90 mm, respectively.

Figure 5 (i) shows the response surface of the interaction between the height of the cone section (E) and the height of the cylinder section (F). When the height of the cylinder section is 40 mm and 50 mm, the sampling efficiency can reach 0.95 and 0.966, and at 60 mm, the sampling efficiency can reach 0.952. As the height of the cone section increases, the sampling efficiency shows an upward trend. When the height of the cylinder section is significant, the sampling efficiency shows a downward trend as the height of the cone section increases.

Parameter optimization

Using the Design Expert response surface optimization method to process data on the dimensions of 54 sets of models, the system automatically seeks the optimal result through regression equations and response surface analysis. The optimization results are shown in Table 5, with the first line being the default optimal result sought by the system.

Table 5

The results after the sand collecting unit have undergone systematic optimization

	A	B	C	D	E	F	Expected value
1	0	1	1	0	1	0	1
2	0	0	1	1	0	1	1
3	0	0	0	0	0	0	1
4	1	0	0	1	-1	0	1
5	1	0	1	0	0	-1	1
6	-1	0	0	1	-1	0	1

Micro Wind Tunnel Testing

The optimal structure of the drainage-type cyclone separation sand sampler unit was determined through simulation experiments, and various components were mechanically processed. Subsequent validation tests were conducted. The test equipment adopts the movable wind erosion wind tunnel and micro wind tunnel of Inner Mongolia Agricultural University to test the sand sampler unit and sand sampler instrument separately. The thermal sensitive velocimeter is used to control the test wind speed accurately, and high-precision electronic scales are used to weigh the sand samples before and after the test accurately. For artificial screening of sand particles with a particle size less than 0.5 millimeters, considering the simulation of actual natural phenomena, the selected sand particles do not require drying treatment.

Prepare 12 sand samples, each weighing 60 g. The sand sampler consists of six sand sampler units. Because the six sand sampler units on the sand sampler have the same structure except for different heights above the ground, one sand sampler unit on the sand sampler is selected for sampling and weighing the sand volume. Four wind speeds of 7 m/s, 9 m/s, 11 m/s, and 13 m/s were used for the test. Three tests were

conducted at each wind speed, and the average of the three tests was taken to ensure the accuracy of the test. After the experiment, the sand samples collected in the sand sampler bag will be weighed using a high-precision electronic scale, and the average value of three experiments will be taken. The experimental device is shown in Figure 5. The gas-solid sampling efficiency values of the drainage type sand sampler unit calculated at four wind speeds of 7 m/s, 9 m/s, 11 m/s, and 13 m/s are 97.43%, 97.55%, 97.71%, and 98.92%, with an average sampling efficiency of 97.95%. The gas-solid sampling efficiency values of traditional-type sand sampler units are 96.54%, 96.82%, 97.24%, and 98.51%, with an average sampling efficiency of 97.32%. The effect of the drainage-type sand sampler unit is better than that of the traditional type sand sampler unit (Fig.6).

Fig. 6 - Miniature wind tunnel test drawing

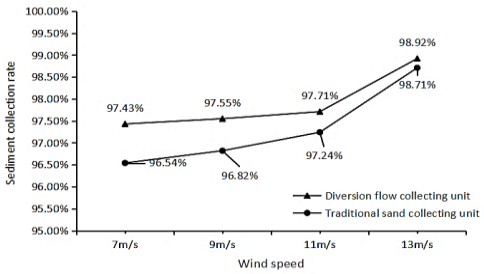

Fig. 7 - Comparison of sampling efficiency between diversion flow and traditional type

The gas-solid sampling efficiency values of the drainage type sand sampler unit calculated at four wind speeds of 7 m/s, 9 m/s, 11 m/s, and 13 m/s are 99.11%, 97.71%, 97.55%, and 97.43%, respectively. The average sampling efficiency is 97.95%, better than the traditional formula with 96.54%, 96.82%, 97.24%, and 98.71%, and the average sampling efficiency is 97.32% (Figure 7). The sampling efficiency of the drainage type and traditional sand sampler units shows a significant upward trend with the increase in wind speed. When the wind speed is low, the difference in sampling efficiency between the drainage type and traditional sand sampler units is more significant and needs to be improved. At the same wind speed, the sampling efficiency of the drainage type is better than that of the traditional type, and the experimental results meet the design expectations.

Wind Erosion Wind Tunnel Test

Conduct wind erosion wind tunnel tests to measure the sand sampler effect. Place the drainage type sand sampler used in micro wind tunnel tests in the groove of the wind erosion wind tunnel (Figure 8). The minimum height of the air inlet of the sand sampler unit from the ground is 20 mm, and the maximum height is 520 mm. Each sand sampler unit is spaced 100 mm apart, making collecting sand at different heights easy. The sand transportation adopts a floor-laying method, and the test sand is divided into 4 parts, with each part of 10000 g laid flat in the wind tunnel channel. Tie plastic bags under the drainage pipe to collect sand samples. Conduct experiments at four wind speeds of 7 m/s, 9 m/s, 11 m/s, and 13 m/s. After the experiment, weigh the sand's weight collected by the sand sampler unit at each height.

Calculate the fitting values of the sand sampler volume for the drainage-type cyclone separation sand sampler at different wind speeds and heights. The larger the determination coefficient R2 and the better its fit, the lower and upper bounds of the integration are taken as the height above the ground. Integrate the sand sampler volume at different heights to obtain the actual sand transport volume. The test research shows that the sand sampler volume of the sand sampler is a power function with the increase of the sampler height, which satisfies the equation 1:

$$q = ax^b \tag{2}$$

where q is the sand concentration at the height of sand sampler, ɑ and b is the coefficient of the equation, x is the height of sand sampler (mm). Actual sand sampler capacity:

$$Q = \int_1^{52} q dx \tag{3}$$

At wind speeds of 7 m/s, 9 m/s, 11 m/s, and 13 m/s, the sand sampler efficiency is 67.19%, 88.36%, 93.46%, and 92.52%, respectively. During the experiment, the wind tunnel wind speed ranged from 9 m/s to 13 m/s, and the sand sampler efficiency varied steadily, with an average value of 91.44%, meeting the design requirements. Moreover, calculate the sampling efficiency of the traditional cyclone separation and sand sampler at wind speeds of 7 m/s, 9 m/s, 11 m/s, and 13 m/s, which are 66.88%, 87.82%, 92.24%, and 91.48%, respectively. During the experiment, the sampling efficiency of the wind tunnel wind speed in the range of 9 m/s to 13 m/s changed smoothly, with an average value of 90.81%. The comparison of sand sampler efficiency of two sand sampler singletons is shown in Figure 9.

Fig. 8 - Wind erosion wind tunnel test drawing

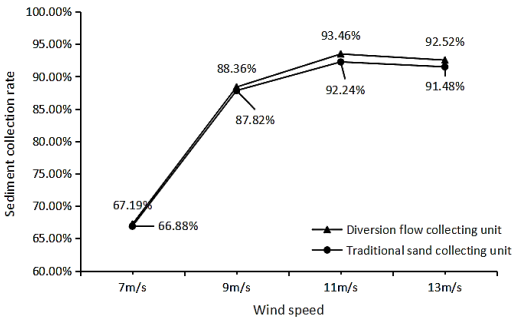

Fig. 9 - Line chart of sampling efficiency

CONCLUSIONS

Grasslands are crucial ecosystems in China, vital for maintaining ecological balance, preventing soil erosion, and conserving water resources. However, due to climate change and human activities, they have suffered significant degradation, with soil wind erosion being a major factor. Accurate monitoring of wind erosion is essential for the protection and restoration of these ecosystems. Dust samplers are key tools for detecting wind erosion, measuring sand transport and flow structure. However, current cyclone-type samplers have limitations in sampling efficiency.

This paper introduced a drainage-type cyclone dust sampler, which added a drainage pipe beneath the cyclone separator to reduce air backflow and improve efficiency. To optimize its design and enhance monitoring accuracy, this study presented the following research efforts:

(1) An Experimental design was conducted on the sampling efficiency of the sand sampler unit of the drainage-type cyclone separation sand sampler using the Box-Behnken response surface analysis method. The sampling efficiency was used as the experimental indicator to establish a mathematical model between the sampling efficiency and experimental factors (inlet wind speed, outlet diameter, exhaust pipe diameter, exhaust pipe insertion depth, cylinder section height, cone section height).

(2) The significance of each factor on the experimental indicators was estimated through model parameters: E>C>A>D>B>F (primary term), CD>DF>BC>AE>CE>AC>EF>AF>BD>BE>BF>CF>AB>AD>DE (interaction term of different factors), D2>E2>F2>B2>C2>A2 (secondary term).

(3) Taking sampling efficiency as the optimization index, the optimal sampling efficiency of the sand sampler unit model was obtained in the experiment when the parameter values were as follows. The cylinder diameter was 60 mm, the cylinder section height was 60 mm, the cone section height was 90 mm, the exhaust pipe diameter was 30 mm, the exhaust pipe interpolation depth was 10 mm, and the sand outlet diameter was 15 mm.

(4) The cyclone separation sand sampler of drainage type performance was tested using wind tunnel tests. The experimental study showed that the average sampling efficiency of the sand sampler was 91.44% at wind speeds of 7 m/s to 13 m/s, indicating good performance. The drainage cyclone separation sand sampler unit obtained in this study provides a good measurement standard for monitoring the degree of land desertification. The sampling efficiency of the sand sampler unit reflects the actual sand concentration in the natural state of wind sand flow, providing a reference for obtaining more accurate and reliable wind sand flow data and improving the current situation of grassland wind erosion. Monitoring grassland degradation and soil erosion by wind with a sand sampler can reflect the real speed change, which provides a reliable theoretical reference for protecting nature and preventing land desertification in China.

ACKNOWLEDGEMENT

The authors were funded for this project by the National Natural Science Foundation of China (NSFC) (No.51869030) and science and technology project of Xinjiang Production and Construction Corps (No.2021CB021).

REFERENCES

[1] Chen, Y. (2018). *Research on Automatic Variable Spraying Technology and Related Parameter Optimization of Spraying Machine Based on Multisource Information (基于多源信息的自动变量喷涂技术及喷涂机相关参数优化研究)*. PhD thesis. Univ. Inner Mongolia agricultural, Hohhot/China.

[2] Cao, A-N; Wu, C-D; Zhang, B; Chen, Z; Jia, W-D; Li, W. (2023). Simulation and Analysis of Spray Barrel Motion for Unmanned spray Vehicles Replacing Pesticides (替代农药的无人喷雾车喷雾筒运动仿真与分析). *Research on Agricultural Mechanization*, Vol. 45(08), pp. 10-17, Heilongjiang/China.

[3] Dumitru, D.; Bălțatu, C.; Marin, E.; Gheorghe, G-V.; Manea, D.; Mateescu, M.; Cismaru, M-E. (2024). Technologies and constructive solutions regarding the inter-row management of vineyard and fruit trees, *INMATEH - Agricultural Engineering* 72(1), pp. 848-860.

[4] Huang, Y; Zhao, M-Q. (2015). Optimization design of cyclone separation sand collector based on numerical simulation and wind tunnel test (基于数值模拟和风洞试验的旋风分离集砂器优化设计). *Transactions of the Chinese Society of Agricultural Engineering*, 31(16): 50-56, Hohhot/China.

[5] He, X-Y; Ma, S-K; Liu, Z-X; Wang, W-D; Shang, S-Q; Li, G-H; Li, H-X. (2024)., Calibration and testing of saline soil parameters based on EDEM discrete element methodology, *INMATEH - Agricultural Engineering* 73(2), pp. 822-833.

[6] Jhang, S-S., Lo, Y-L., Le, T-N. (2019). Systematic modeling approach for analyzing the powder flow and powder energy absorptivity in direct energy deposition system. *Int J Adv Manuf Technol* 105(1-4), 1765–1776.

[7] Khan Sher Afghan, Ibrahim Omar Mohamed, Aabid Abdul. (2021). CFD analysis of compressible flows in a convergent-divergent nozzle. *Materials Today*: Proceedings,46(P7): 2835-2842.

[8] Liu, H-Y; Chen, Z; Hou, Z-F; Tong, X; Zong, Z-Y. (2019). Development and test of soil wind erosion real-time monitoring system based on GPRS (基于 GPRS 的土壤风蚀实时监测系统开发与试验). *Transactions of the Chinese Society of Agricultural Engineering*, 35(05): 163-172, Hohhot/China.

[9] Li, H-S. (2022). Design of cyclone classification control system based on Fluent. *Computer measurement and control*, 30(04): 128-133+154.

[10] Li, B-P; Chen, X-C; Ying, Z; Li, J-R; Zhang C-X. (2022). Wind tunnel simulation of different soil moisture conditions on surface wind erosion in desert steppe of Inner Mongolia (内蒙古荒漠草原不同土壤湿度条件对地表风蚀的风洞模拟). *Arid area resources and environment*, 36 (09):126-132, Hohhot/China.

[11] Petrichenko M.R., Sergeev V.S., Nemova D, Kotov E.V., Tarasova D.S. (2020). CFD simulation of the convective flows in the vertical caverns. *Magazine of Civil Engineering*, 8 (92): 172.

[12] Patil Vaibhav D. Pise Gargee, Nandgaonkar Milankumar R. (2022). Analysis of Phase Change Material used as Thermal Energy Storage Unit in Catalytic Converter. *IOP Conference Series: Materials Science and Engineering*,1248(1).

[13] Song, T. (2016). *Study on the internal flow field characteristics of the combined automatic sand collector with shunt hedge and multistage expansion (分流绿篱多级膨胀组合式自动集砂器内部流场特性研究)*. Master's thesis. Inner Mongolia Agricultural University, Hohhot /China

[14] Song, T; Meng, X-J; Bian, B-C. (2018). Design parameter analysis of diverging hedge and multi-stage expansion automatic sand collection box (分流绿篱与多级膨胀式自动集沙箱设计参数分析). *Chinese Journal of Agricultural Mechanization2018*, 39 (12): 83-87, Hohhot/China.

[15] Xu, B; Cui, Q-L; Zheng, D-C. (2023). Improvement design and simulation analysis on centrifugal disc organic fertilizer spreader, *INMATEH - Agricultural Engineering* 70(2), pp. 329-336.

[16] Yang, Q. (2021). *Numerical simulation and optimization of gas-solid flow characteristics in a sand collector (集砂器内气固流动特性数值模拟与优化)*, Master's thesis. Wuhan University of Technology, Wuhan/China.

[17] Yan, M; Jin, A-F; Gao, W-X. (2024). Optimization of joint sand barrier spacing and characterization of wind-sand flow study based on CFD numerical simulation, *INMATEH - Agricultural Engineering* 73(2), pp. 855-869.

[18] Zhang, F; Shao, W; Zhao, S; Zhu, J; Li, P. (2023). Simulation test and verification of material conveying for small and medium-sized air suction jujube picking machine based on CFD DEM coupling, *INMATEH - Agricultural Engineering* 71(3), pp. 535-547.